No.85 **Nov. 2021**

ISSN 0917-2211

Variable Star Bulletin

Periodic modulations during a long outburst in V363 Lyr

Taichi Kato[1]

[1] Department of Astronomy, Kyoto University, Sakyo-ku, Kyoto 606-8502, Japan

tkato@kusastro.kyoto-u.ac.jp

Received 2021 Nov. 14

Abstract

I analyzed the Kepler long and short cadence data of V363 Lyr. A period of 0.185723(8) d was persistently detected and this is identified as the orbital period. V363 Lyr showed one long outburst accompanied by an "(embedded) precursor" during Kepler observations and modulations with a period of 0.1956(2) d, longer than the orbital one, were detected during this outburst. There are two possible interpretations of this period. The first one is superhumps despite that V363 Lyr is far above the period gap. This interpretation requires an evolved, undermassive secondary enabling a low mass ratio of q=0.15. The evolution of this long-period variations, however, does not follow the standard evolution of superhumps. The second one is that the precursor occurred when the disk reached the tidal truncation radius, as inferred from observations of IW And stars. In this case, the long-period variations could be interpreted as a variable stream impact on a precessing eccentric disk, which may have been formed by disturbances at the tidal truncation radius. This might lead to effective removal of the angular momentum which resulted in 0.3–0.4 mag brightening following the precursor. The fractional period excess suggests that q is just above the stability limit of the 3:1 resonance. In either cases, the nature of the secondary and the mass ratio need to be verified by spectroscopic observations.

1 Introduction

V363 Lyr is a dwarf nova discovered by Hoffmeister (1967). Galkina and Shugarov (1985) studied this object photographically. Although both authors suggested high frequency of outbursts, the interval (∼21.4 d) was first confidently measured by CCD observations by Kato et al. (2001). Liu et al. (1999) spectroscopically confirmed this object to be a cataclysmic variable (CV). This object is included in the Kepler field (Borucki et al. 2010; Koch et al. 2010) and was observed as a Kepler target as KIC 7431243. Ramsay et al. (2014) reported an analysis of the 5.2 d segment and detected two periods of 4.68 hr and 4.47 hr, which I will discuss in this paper.

2 Data Analysis

The data analysis was performed practically in the same way as in Osaki and Kato (2013a,b): I used two-dimensional Fourier analysis for detecting the signals and examined $O-C$ diagrams to detect variation of the periods.

Two sets of Kepler data for V363 Lyr are publicly available: quarter 15 (Q15) short cadence (SC) and Q16 long cadence (LC) data. Since the Q15 observations (in quiescence) covered only for 5.3 d, I primarily used this quarter for confirming the period detected in Q16. The Q16 data contained five short outbursts and one long outburst.

3 Results

3.1 Identification of two periods

I present the result of period analysis only around the frequencies of these periods. There is no candidate frequency outside this frequency region. The results of the Fourier analysis is shown in figure 1. Two major signals were present. These signals corresponds to the periods detected by Ramsay et al. (2014).

I examined the stability of the signal at 5.38 c/d. Almost all the segments (4 d in width), both in quiescence and in outburst, showed the constant phase and almost constant amplitude (in flux) of this 5.38-c/d signal (figure 2). I conclude that this signal was coherent during the Kepler observation, and identified it to be the orbital period ($P_{\rm orb}$). A phase dispersion minimization (PDM: Stellingwerf 1978) analysis of the combined data set of Q15 and Q16 yielded a period of 0.185723(8) d (figure 3). The error was estimated by methods of Fernie (1989) and Kato et al. (2010).

A two-dimensional Fourier analysis (figure 1) clearly indicates that another signal around frequencies 5.0–5.2 c/d was especially strong around the long outburst. Since the frequency of this signal is lower (i.e. the period is longer) than that of $P_{\rm orb}$. Hereafter I call this signal $\rm P_+$. A two-dimensional PDM analysis is also shown in figure 1. In the case of V363 Lyr, PDM analysis gave a better result than least absolute shrinkage and selection operator (Lasso: Tibshirani 1996; Kato and Uemura 2012; Kato and Maehara 2013) analysis employed in Osaki and Kato (2013b) due to the non-sinusoidal nature of the signal and small number of points in the LC data. The resolution of PDM analysis is intermediate between Fourier transform and Lasso analysis, and this result can be treated as a slightly degraded version of Lasso analysis presented in Osaki and Kato (2013b) [see also an application of a two-dimensional PDM analysis to superhumps in Kato et al. (2021b)]. It looks like that $\rm P_+$ was sometimes weakly excited outside the long outburst. No evidence of the negative superhump was detected.

3.2 Development of $\rm P_+$

The long outburst had a shoulder (precursor) followed by a brighter outburst. This phenomenon in SS Cyg stars is also referred to as an "embedded precursor" by Cannizzo (2012). During the precursor, humps recurring with $P_{\rm orb}$ were recorded. After BJD 2456352 (two days after the peak), $\rm P_+$ humps appeared.

I measured the times of maxima of these humps in the light curve by the template fitting method described in Kato et al. (2009) after removing the trend of the outburst by locally-weighted polynomial regression (LOWESS: Cleveland 1979). I used the raw light curve (without subtraction of the orbital signal) in figure 4. The times of maxima are listed in table 1. As shown in figure 4, the variations during the precursor can be identified as the orbital signal. After the precursor, the object brightened by 0.3–0.4 mag. No clearly periodic variations were detected for 2 d. The amplitudes of $\rm P_+$ were small ($\sim$0.04 mag) and there was no significant variation of the period. The profile of $\rm P_+$ was slightly asymmetric (figure 6).

4 Discussion

4.1 Comparison with superhumps in SU UMa stars

As we have seen, V363 Lyr showed both the orbital signal and the $\rm P_+$ signal longer than $P_{\rm orb}$ during the long, bright outburst. These $\rm P_+$ variations may look similar to superhumps in SU UMa stars, which have periods a few percent longer than $P_{\rm orb}$ and are considered to arise from the precession of an eccentric accretion disk whose deformation is excited by the 3:1 resonance (Whitehurst 1988; Hirose and Osaki 1990; Lubow 1991).

There are, however, a number of features different from superhumps in ordinary SU UMa stars. They are:

- The orbital period is too long [0.185723(8) d] for a typical SU UMa star [see e.g. Warner (1995) for classical statistics], although some long-$P_{\rm orb}$ dwarf novae are classified as SU UMa stars (see e.g. Kato et al. 2021a).
- The ratio between the durations of the long outburst (12 d for the entire outburst, 6 d after the long period appeared) and other outbursts (5 d) is small compared to other SU UMa stars.
- Superhumps in SU UMa stars usually show $O-C$ variations (Kato et al. 2009). $\rm P_+$ in V363 Lyr, however, did not show such a variation.
- In many SU UMa stars, superhumps start to appear during the precursor (Osaki and Kato 2013a,b). In V363 Lyr, $\rm P_+$ appeared much later (2 d after the end of the precursor).

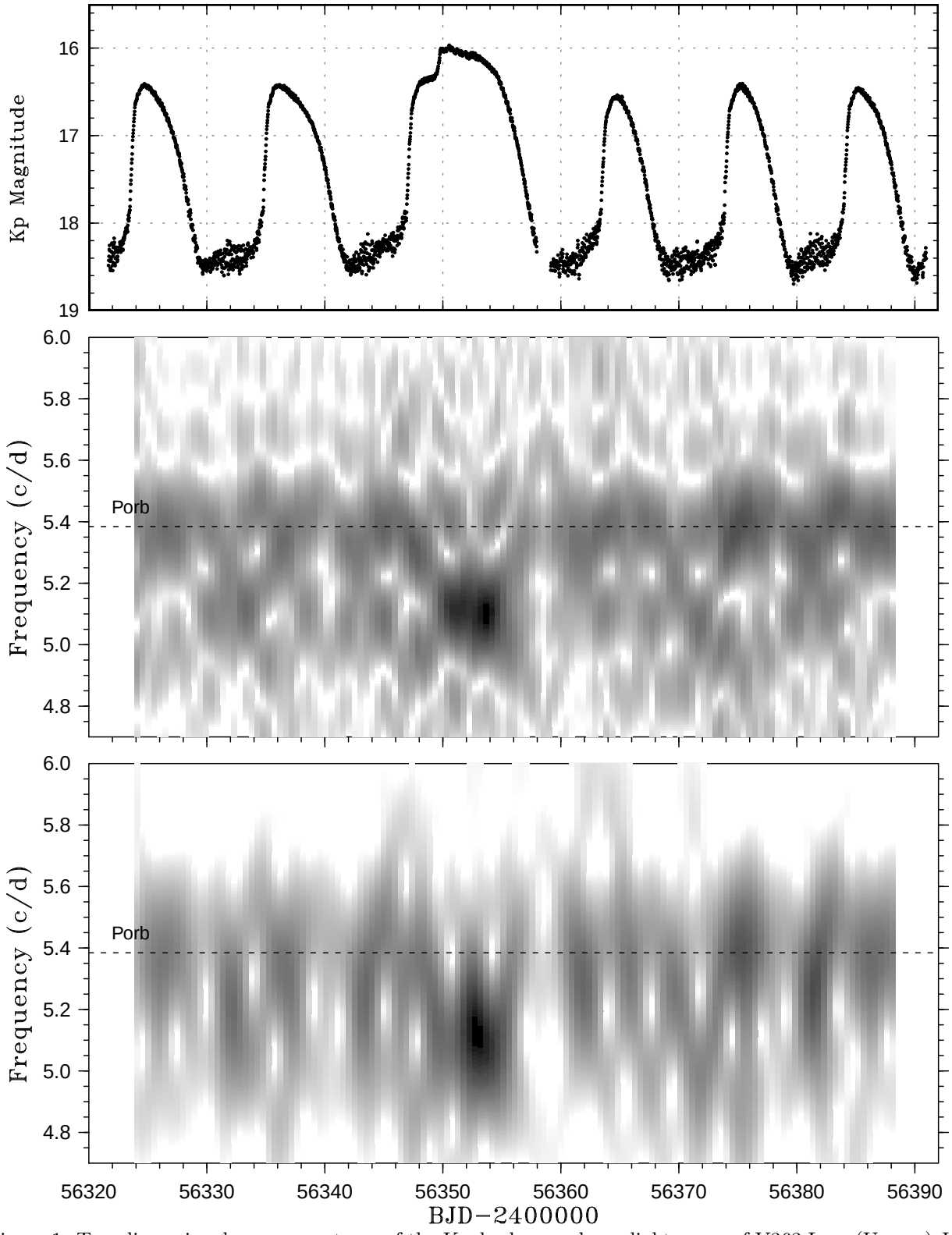

Figure 1: Two-dimensional power spectrum of the Kepler long cadence light curve of V363 Lyr. (Upper:) Kepler Light curve. (Middle:) Power spectrum. The width of the sliding window and the time step used are 5 d and 0.5 d, respectively. A Hanning window function was used. A signal (P_+) with a period longer than $P_{\rm orb}$ appeared during the long outburst. (Lower) Two-dimensional PDM analysis. The width of the sliding window and the time step used are 5 d and 0.5 d, respectively. Dark colors represent signals (lower θ in the PDM statistics). The orbital signal was present except during the long outburst. The signal of P_+ was strongest during the long outburst.

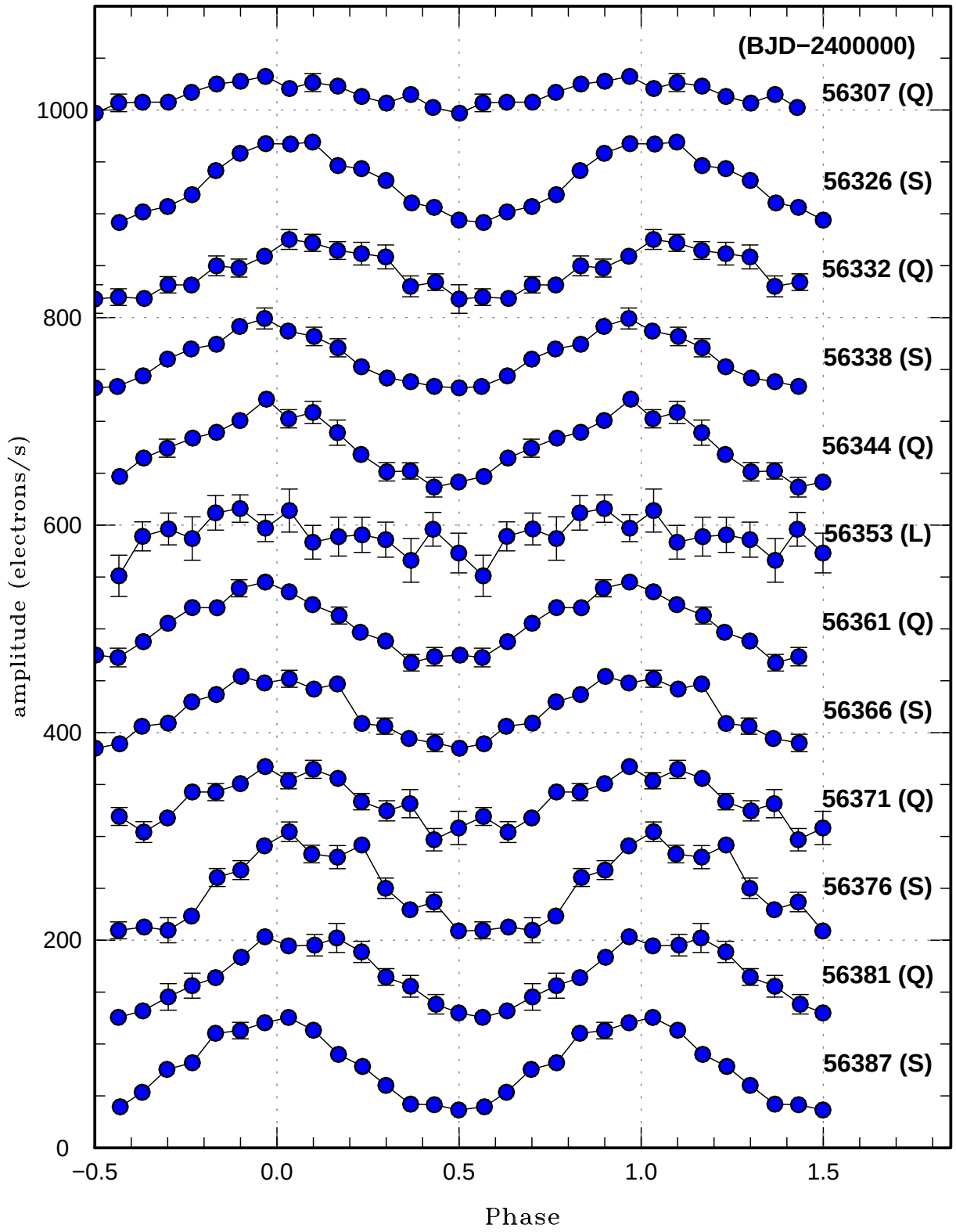

Figure 2: Variation of the profile of the 5.38-c/d signal. Each phase-averaged light curve was constructed from 4-d Kepler observations centered on the dates shown in the figure. The phase= 0 and period were defined as BJD 2456351.979 and 0.185723 d, respectively. The days 56307, 56332, 56344, 56361, 56371 and 56381 correspond to quiescence (Q in the figure); the days 56326, 56338, 56366, 56376 and 56387 correspond to short outbursts (S). The day 56353 corresponds to the long outburst (L). Only except during the long outburst, the 5.38-c/d signal was detected with a constant phase and almost constant amplitudes (in flux).

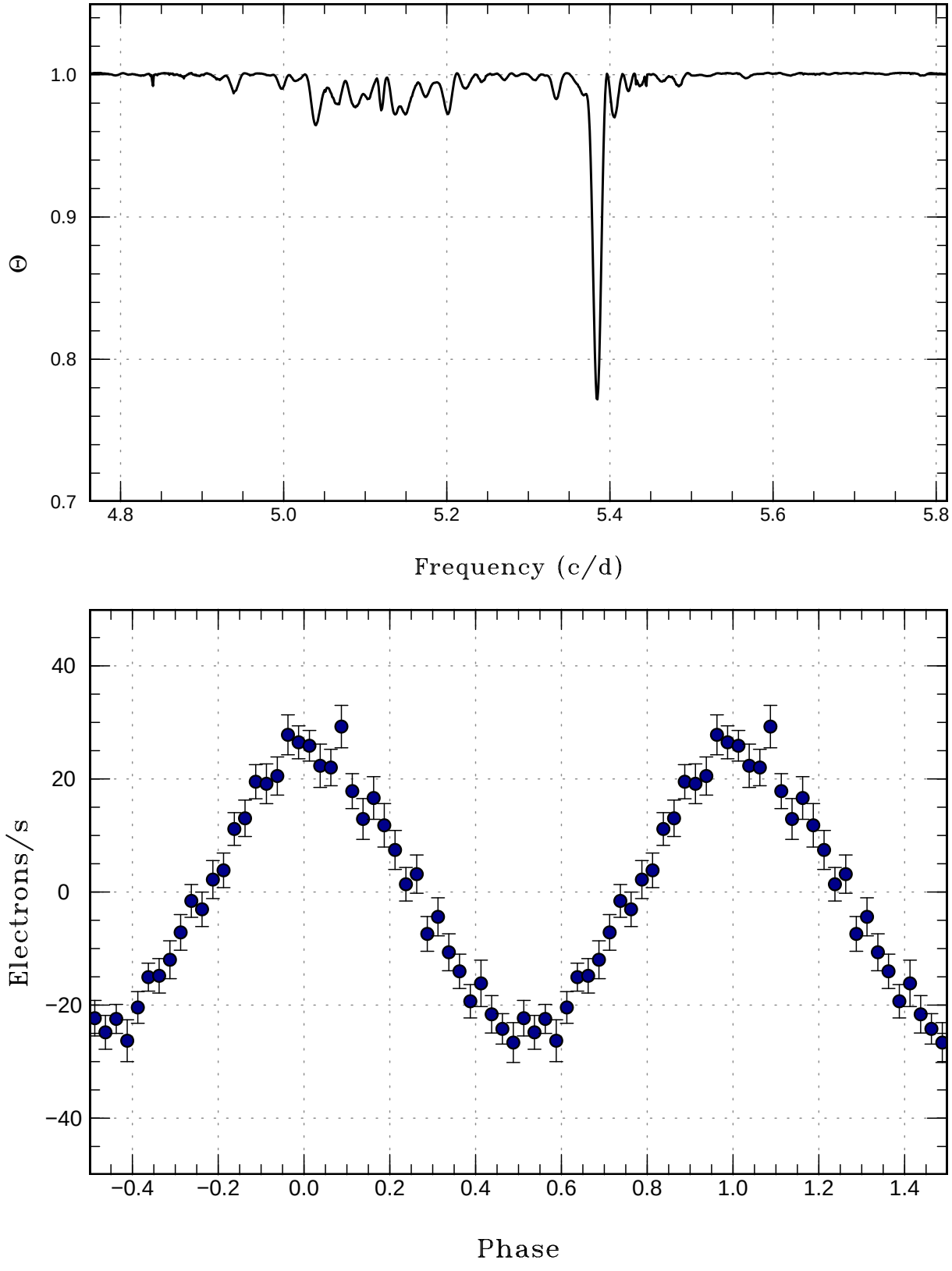

Figure 3: PDM analysis of V363 Lyr of the entire data. Upper: PDM analysis. The sharp signal at 0.18572 d is $P_{\rm orb}$. Lower: mean profile of the orbital signal.

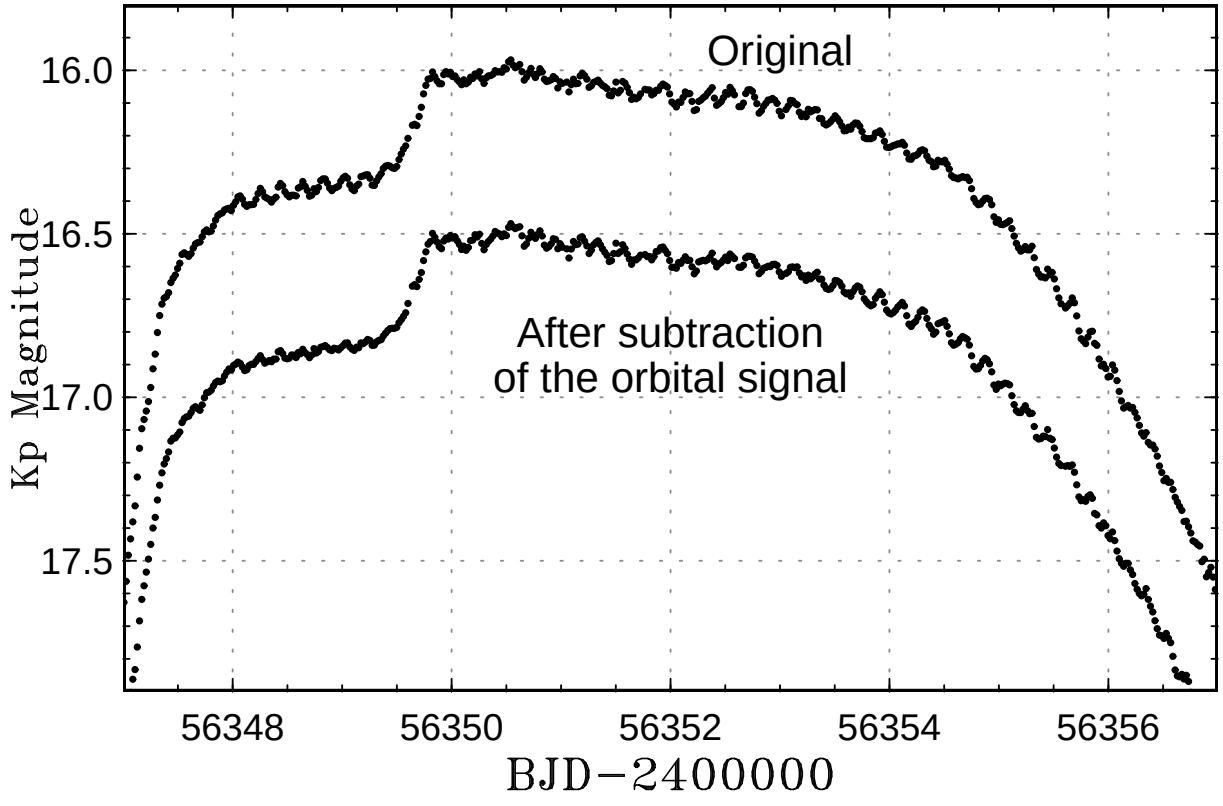

Figure 4: Long outburst of V363 Lyr. The light curve of original observations (upper) and the light curve after subtraction (in flux) of the mean orbital signal are shown. The latter light curve was shifted by 0.5 mag. This long outburst had a shoulder (precursor) followed by a brighter outburst. Semi-regular variations were visible during the precursor, which can be interpreted as the orbital signal. Two days after the object reached the peak brightness, P_+ humps appeared.

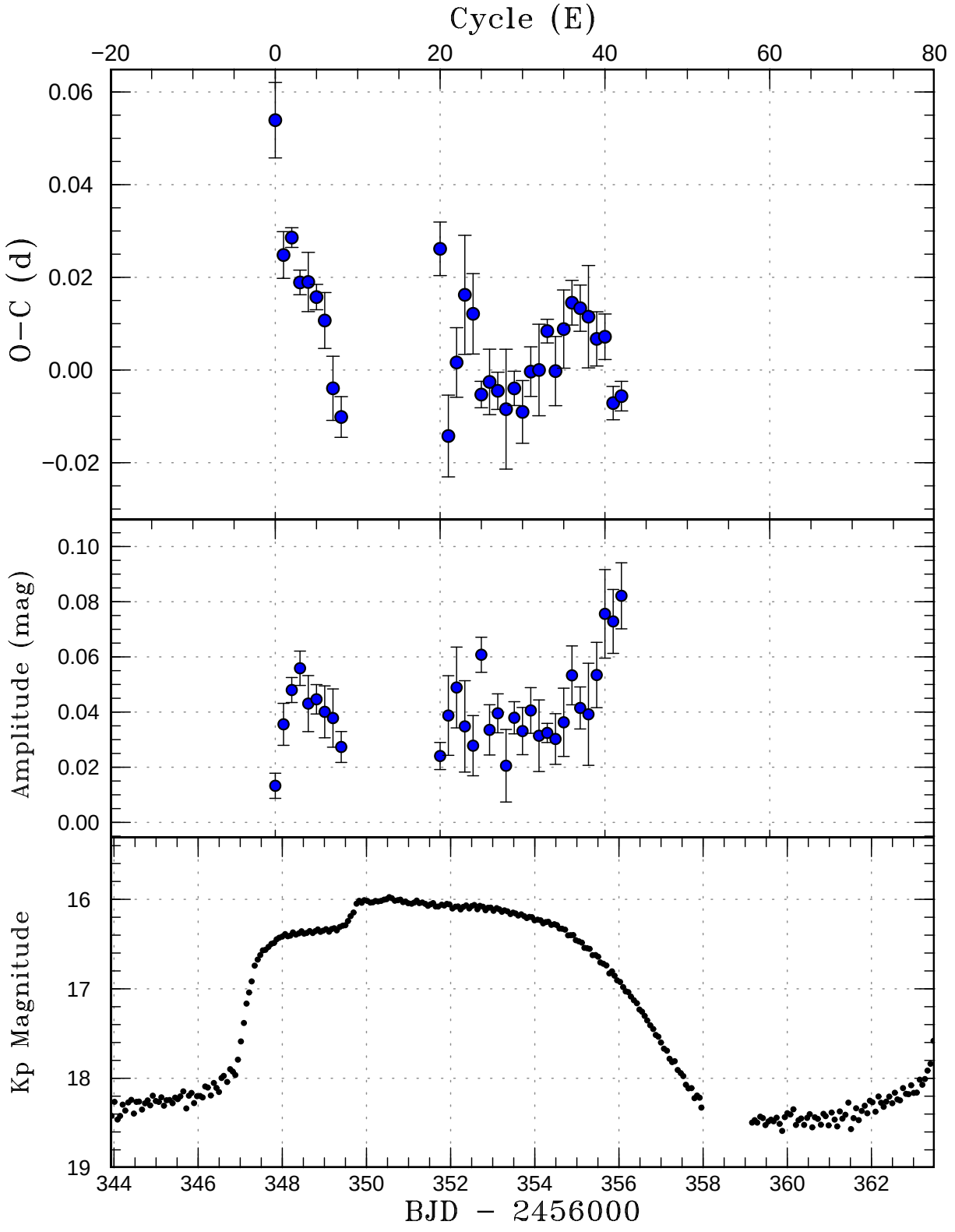

Figure 5: $O-C$ diagram of humps during the long outburst in V363 Lyr. (Upper:) $O-C$ diagram. The maxima for $E \leq 8$ refer to the orbital signal (see text). P_+ appeared around $E = 20$. I used a period of 0.19585 d for calculating the $O-C$ residuals. (Middle:) Amplitudes of P_+ humps. (Lower:) Light curve. The data were binned to 0.065 d.

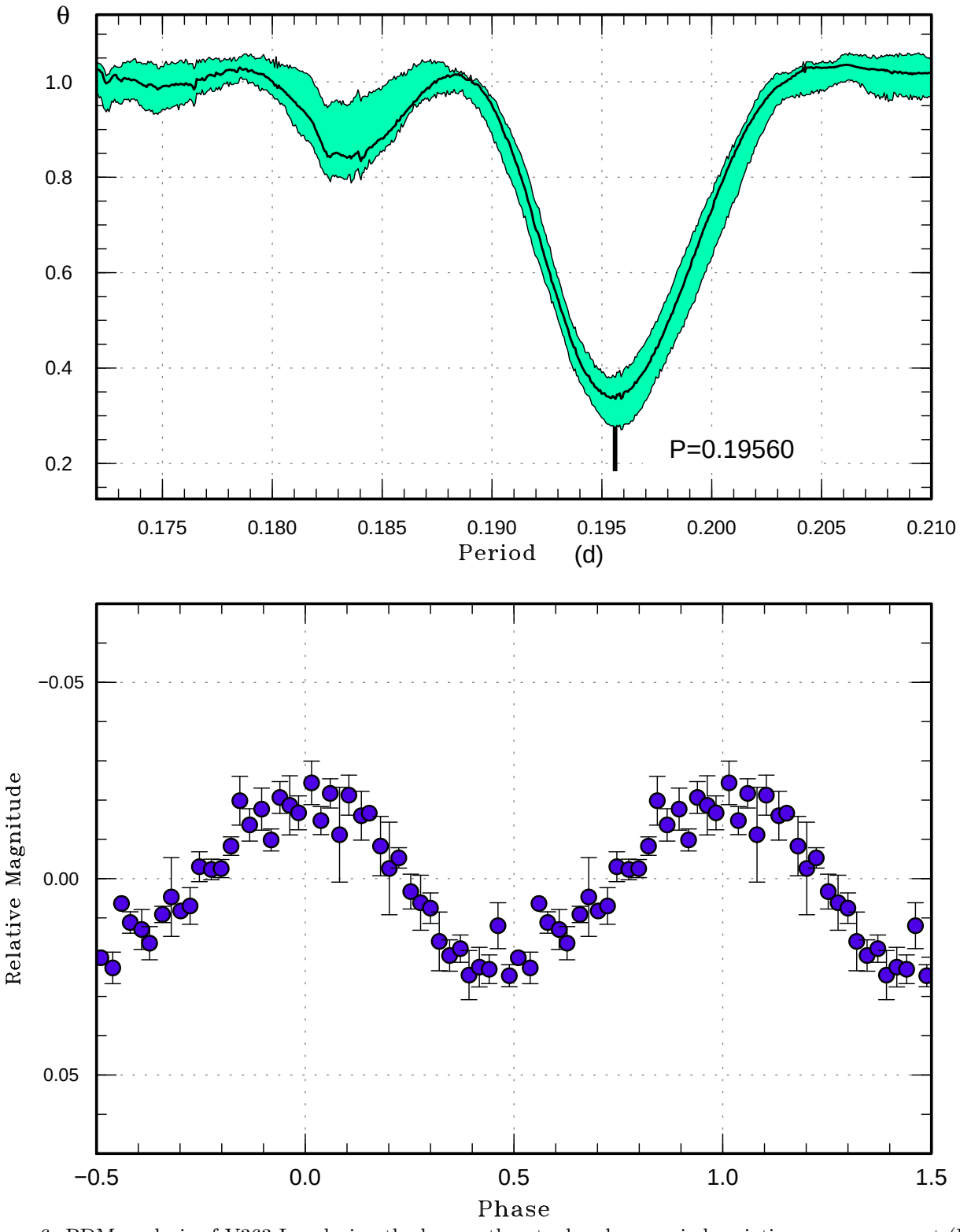

Figure 6: PDM analysis of V363 Lyr during the long outburst when long-period variations were apparent (BJD 2456352–2456356.5). Upper: PDM analysis. I analyzed 100 samples which randomly contain 50% of observations and the result is shown as a form of 90% confidence intervals in the resultant PDM θ statistics. The signal at 0.1956 d corresponds to P_+. Lower: mean profile of P_+ variations.

Table 1: Times of maxima in V363 Lyr during the long outburst

E	max*	error	$O-C^{\dagger}$	$N^{\ddagger}$
0	56347.8869	0.0081	0.0351	8
1	56348.0537	0.0050	0.0065	7
2	56348.2533	0.0021	0.0107	7
3	56348.4395	0.0027	0.0016	8
4	56348.6354	0.0064	0.0022	8
5	56348.8280	0.0027	−0.0006	7
6	56349.0188	0.0060	−0.0051	8
7	56349.2000	0.0069	−0.0193	8
8	56349.3897	0.0044	−0.0249	7
20	56351.7762	0.0058	0.0175	7
21	56351.9316	0.0088	−0.0224	8
22	56352.1433	0.0075	−0.0060	8
23	56352.3538	0.0128	0.0091	8
24	56352.5455	0.0087	0.0055	6
25	56352.7240	0.0029	−0.0114	8
26	56352.9225	0.0071	−0.0082	8
27	56353.1165	0.0040	−0.0096	7
28	56353.3083	0.0129	−0.0131	7
29	56353.5087	0.0037	−0.0081	8
30	56353.6995	0.0068	−0.0126	8
31	56353.9040	0.0054	−0.0034	8
32	56354.1002	0.0099	−0.0026	8
33	56354.3044	0.0026	0.0063	8
34	56354.4917	0.0075	−0.0018	8
35	56354.6966	0.0084	0.0078	8
36	56354.8981	0.0048	0.0140	8
37	56355.0928	0.0050	0.0133	8
38	56355.2868	0.0110	0.0120	7
39	56355.4779	0.0058	0.0077	8
40	56355.6742	0.0049	0.0087	7
41	56355.8557	0.0036	−0.0052	7
42	56356.0531	0.0032	−0.0031	7

*BJD−2400000.

†Against max $= 2456347.8519 + 0.195341E$.

‡Number of points used to determine the maximum.

4.2 Can P_+ be growing superhumps?

In many SU UMa-type dwarf novae, superhumps start to appear during the precursor (if there is a precursor) or a few to several days after the start of the superoutburst (if there is no precursor). This reflects when the 3:1 resonance starts to develop (Osaki 2005). During this growing phase of superhumps, superhump periods ($P_{\rm SH}$) are longer and this phase is referred to as stage A (Kato et al. 2009). It is interpreted that during the growing phase of superhumps, the eccentric part of the disk is confined to the region near the 3:1 resonance (Osaki and Kato 2013b; Kato and Osaki 2013) and that the period reflects the dynamical precession rate at the 3:1 resonance. As the region of the eccentric part reaches the inner part of the disk, the pressure effect slows down the precession rate (stage B). In many SU UMa-type dwarf novae, stage B superhumps are seen near the peaks of superoutbursts.

P_+ in V363 Lyr has a period of 0.1956(2) d (figure 6), which is 5.3% longer than $P_{\rm orb}$. This period corresponds to a fractional superhump excess in frequency $\epsilon^* \equiv 1 - P_{\rm orb}/P_{\rm SH} = 0.0514(10)$. If we consider that P_+ variations in V363 Lyr reflect the dynamical precession rate at the 3:1 resonance, this value corresponds to a mass ratio of q=0.152(3) (Kato and Osaki 2013). The mass of the secondary inferred from this mass ratio is too small for an object with $P_{\rm orb}$ =0.18572 d. The mass, M_V and M_K ofthe secondary for this period on the standard evolutionary sequence of CVs are $0.39M_\odot$, +10.2 and +5.9, respectively (Knigge 2006). Even a Chandrasekhar-mass white dwarf gives q=0.28, which cannot explain the observation.

There remains a possibility that the secondary in V363 Lyr is undermassive for $P_{\rm orb}$. Such a system should have an evolved secondary such as QZ Ser (Thorstensen et al. 2002), CRTS J134052.1+151341 (Thorstensen 2013) and ASASSN-18aan (Wakamatsu et al. 2021). The quiescent absolute magnitudes of V363 Lyr are M_V=+7.5 and M_K=+4.4 [using 2MASS (Cutri et al. 2003) and Gaia parallax (Gaia Collaboration et al. 2021)]. These values are brighter than those of main-sequence stars on the standard evolutionary sequence of CVs, and the secondary in V363 Lyr may indeed be evolved. For comparison, quiescent absolute magnitudes are M_V=+10.5 and M_K=+7.2 for QZ Ser, M_V=+8.4 and M_K=+5.9 for CRTS J134052.1+151341 and M_V=+8.4 and M_K=+6.0 for ASASSN-18aan. If the secondary is indeed evolved in V363 Lyr, P_+ might be attributed to superhumps arising from the 3:1 resonance. If this is the case, the difference in the behavior of superhumps from other SU UMa stars would require an additional explanation since the corresponding q value is normal for an SU UMa star and textbook evolution of superhumps is expected. Spectroscopic determination of the secondary type and radial-velocity measurements are needed.

4.3 Could P_+ be stream impact on a precessing eccentric disk?

Since P_+ was seen during the middle-to-late phase of the outburst, this variation might be attributed to (traditional) late superhumps (Haefner et al. 1979; Vogt 1983; van der Woerd et al. 1988), which arise from the stream impact on an eccentric disk.

The dynamical precession rate of an eccentric disk can be obtained by the method in Hirose and Osaki (1990); Kato and Osaki (2013) and the disk radius can be estimated by equating the theoretical precession rate with the observed ϵ^*. The results for various q values are listed in table 2. I used the formula of the tidal truncation radius

$$r_{\rm tidal} = \frac{0.60}{1+q} \tag{1}$$

in Paczyński (1977). and Lubow-Shu (or circularization) radius

$$r_{\rm LS} = 0.488 q^{-0.464} \tag{2}$$

from Lubow and Shu (1975). The value q=0.15 corresponds to subsection 4.2 (assuming that P_+ is growing or stage A superhumps). The values q=0.25 or q=0.30 correspond to the limit of the 3:1 tidal instability. The value q=0.476 corresponds to a secondary star on the standard evolutionary sequence of CVs (Knigge 2006) and an average-mass white dwarf $0.82M_\odot$ in CVs (Zorotovic et al. 2011).

In cases for $q < 0.30$ the radius of the 3:1 resonance is inside $r_{\rm tidal}$ and the tidal instability due to the 3:1 resonance can occur. In these cases, an eccentric disk is expected to form by the tidal instability and the identification P_+ as (traditional) late superhumps is possible. This interpretation, however, requires an explanation why ordinary superhumps before the appearance of late superhumps were not observed. In all cases, the estimated radii are far outside $r_{\rm LS}$ and they are achievable. For $q > 0.30$, however, eccentric deformation of the disk by the 3:1 resonance is not expected and there is a need for a different mechanism.

Table 2: Disk radius estimated from the precession rate

q	Disk radius*	Truncation radius*	Radius of 3:1 resonance*	Lubow-Shu radius*
0.15	0.462	0.52	0.459	0.118
0.20	0.413	0.50	0.453	0.103
0.25	0.377	0.48	0.447	0.093
0.30	0.348	0.46	0.441	0.085
0.35	0.325	0.44	0.435	0.079
0.476†	0.283	0.41	0.422	0.069

*Unit: binary separation.

†Assuming a standard secondary and an average mass white dwarf.

4.4 Possible deformation of the disk for a high-q system

If the true mass ratio is too large to hold the 3:1 resonance within the tidal truncation radius, V363 Lyr is not an SU UMa star. Kato and Hambsch (2021) recently proposed an interpretation that embedded precursors in long outbursts of SS Cyg stars may correspond to a phenomenon when the disk radius reaches the tidal truncation radius. This interpretation originated from direct observations of the variation of the disk radius (M. Shibata et al. in preparation) in an IW And star (Simonsen 2011; Kato 2019). If this is indeed the case in the precursor in V363 Lyr, P_+ may be a previously undescribed phenomenon which is excited when the disk reaches the tidal truncation radius. In IW And stars, standstills are terminated by brightening and this would require a mechanism of effective removal of angular momentum at the tidal truncation radius (see Kimura et al. 2020; Kato et al. 2021b; M. Shibata et al. in preparation). It would not be surprising if intersections of orbits in the disk near the tidal truncation radius (Paczyński 1977) cause disturbances and lead to eccentric deformation of the disk (which is desired for the late-superhump type interpretation) and effective removal of the angular momentum. As seen in table 2, the estimated disk radius is much smaller than $r_{\rm tidal}$ for larger q values. This mechanism to produce P_+ would only be acceptable in V363 Lyr for a narrow range of q which does not allow the 3:1 resonance to occur but enables the disk radius sufficiently close to $r_{\rm tidal}$. Brightening by 0.3–0.4 mag after the precursor in V363 Lyr is probably the result of effective removal of the angular momentum (just as in superoutburst in SU UMa stars, Osaki 1989), and P_+ observed in V363 Lyr could be a manifestation of the disturbances around the tidal truncation radius.

Acknowledgments

I thank the Kepler Mission team and the data calibration engineers for making Kepler data available to the public. This work was supported by JSPS KAKENHI Grant Number 21K03616.

References

Borucki, W. J. et al. (2010) Kepler planet-detection mission: Introduction and first results. *Science* **327**, 977

Cannizzo, J. K. (2012) The shape of long outbursts in U Gem type dwarf novae from AAVSO data. *ApJ* **757**, 174

Cleveland, W. S. (1979) Robust locally weighted regression and smoothing scatterplots. *J. Amer. Statist. Assoc.* **74**, 829

Cutri, R. M. et al. (2003) 2MASS All Sky Catalog of point sources (NASA/IPAC Infrared Science Archive)

Fernie, J. D. (1989) Uncertainties in period determinations. *PASP* **101**, 225

Gaia Collaboration et al. (2021) Gaia Early Data Release 3. summary of the contents and survey properties. *A&A* **649**, A1

Galkina, M. P., & Shugarov, S. Yu. (1985) Study of 11 stars in Lyra. *Perem. Zvezdy* **22**, 225

Haefner, R., Schoembs, R., & Vogt, N. (1979) The outbursts of the dwarf nova VW Hydri – a comparative study of short and long eruptions. *A&A* **77**, 7

Hirose, M., & Osaki, Y. (1990) Hydrodynamic simulations of accretion disks in cataclysmic variables – superhump phenomenon in SU UMa stars. *PASJ* **42**, 135

Hoffmeister, C. (1967) Mitteilungen über neuentdeckte veränderliche Sterne. *Astron. Nachr.* **289**, 205

Kato, T. (2019) Three Z Cam-type dwarf novae exhibiting IW And-type phenomenon. *PASJ* **71**, 20

Kato, T., & Hambsch, F.-J. (2021) On the nature of embedded precursors in long outbursts of SS Cyg stars as inferred from observations of the IW And star ST Cha. *VSOLJ Variable Star Bull.* **83**, (arXiv:2110.10321)

Kato, T. et al. (2009) Survey of period variations of superhumps in SU UMa-type dwarf novae. *PASJ* **61**, S395

Kato, T. et al. (2021a) ASASSN-19ax: SU UMa-type dwarf nova with a long superhump period and post-superoutburst rebrightenings. *VSOLJ Variable Star Bull.* **84**, (arXiv:2111.01304)

Kato, T., & Maehara, H. (2013) Analysis of Kepler light curve of the novalike cataclysmic variable KIC 8751494. *PASJ* **65**, 76

Kato, T. et al. (2010) Survey of Period Variations of Superhumps in SU UMa-Type Dwarf Novae. II. The Second Year (2009-2010). *PASJ* **62**, 1525

Kato, T., Nogami, D., Baba, H., & Masuda, S. (2001) Outburst cycle of V363 Lyr. *IBVS* **5118**

Kato, T., & Osaki, Y. (2013) New method to estimate binary mass ratios by using superhumps. *PASJ* **65**, 115

Kato, T. et al. (2021b) BO Ceti: Dwarf nova showing both IW And and SU UMa-type features. *PASJ* in press (arXiv:2106.15028)

Kato, T., & Uemura, M. (2012) Period analysis using the Least Absolute Shrinkage and Selection Operator (Lasso). *PASJ* **64**, 122

Kimura, M., Osaki, Y., & Kato, T. (2020) KIC 9406652: A laboratory of the tilted disk in cataclysmic variable stars. *PASJ* **72**, 94

Knigge, C. (2006) The donor stars of cataclysmic variables. *MNRAS* **373**, 484

Koch, D. G. et al. (2010) Kepler mission design, realized photometric performance, and early science. *ApJ* **713**, L79

Liu, Wu., Hu, J. Y., Zhu, X. H., & Li, Z. Y. (1999) Spectroscopic confirmation of 55 northern and equatorial cataclysmic variables. I. 27 confirmed cataclysmic variables. *ApJS* **122**, 243

Lubow, S. H. (1991) A model for tidally driven eccentric instabilities in fluid disks. *ApJ* **381**, 259

Lubow, S. H., & Shu, F. H. (1975) Gas dynamics of semidetached binaries. *ApJ* **198**, 383

Osaki, Y. (1989) A model for the superoutburst phenomenon of SU Ursae Majoris stars. *PASJ* **41**, 1005

Osaki, Y. (2005) The disk instability model for dwarf nova outbursts. *Proc. Japan Acad. Ser. B* **81**, 291

Osaki, Y., & Kato, T. (2013a) The cause of the superoutburst in SU UMa stars is finally revealed by Kepler light curve of V1504 Cygni. *PASJ* **65**, 50

Osaki, Y., & Kato, T. (2013b) Study of superoutbursts and superhumps in SU UMa stars by the Kepler light curves of V344 Lyrae and V1504 Cygni. *PASJ* **65**, 95

Paczyński, B. (1977) A model of accretion disks in close binaries. *ApJ* **216**, 822

Ramsay, G. et al. (2014) RATS-Kepler – a deep high-cadence survey of the Kepler field. *MNRAS* **437**, 132

Simonsen, M. (2011) The Z CamPaign: Year 1. *J. American Assoc. Variable Star Obs.* **39**, 66

Stellingwerf, R. F. (1978) Period determination using phase dispersion minimization. *ApJ* **224**, 953

Thorstensen, J. R. (2013) CSS J134052.0+151341: A cataclysmic binary star with a stripped, evolved secondary. *PASP* **125**, 506

Thorstensen, J. R., Fenton, W. H., Patterson, J. O., Kemp, J., Halpern, J., & Baraffe, I. (2002) QZ Serpentis: A dwarf nova with a 2-hour orbital period and an anomalously hot, bright secondary star. *PASP* **114**, 1117

Tibshirani, R. (1996) Regression shrinkage and selection via the lasso. *J. R. Statistical Soc. Ser. B* **58**, 267

van der Woerd, H., van der Klis, M., van Paradijs, J., Beuermann, K., & Motch, C. (1988) Observations of the late superhump in VW Hydri. *ApJ* **330**, 911

Vogt, N. (1983) VW Hydri revisited – conclusions on dwarf nova outburst models. *A&A* **118**, 95

Wakamatsu, Y. et al. (2021) ASASSN-18aan: An eclipsing SU UMa-type cataclysmic variable with a 3.6-hr orbital period and a late G-type secondary star. *PASJ* **73**, 1209

Warner, B. (1995) Cataclysmic Variable Stars (Cambridge: Cambridge University Press)

Whitehurst, R. (1988) Numerical simulations of accretion disks. I - superhumps - a tidal phenomenon of accretion disks. *MNRAS* **232**, 35

Zorotovic, M., Schreiber, M. R., & Gänsicke, B. T. (2011) Post common envelope binaries from SDSS. XI. the white dwarf mass distributions of CVs and pre-CVs. *A&A* **536**, A42

VSOLJ
c/o Keiichi Saijo National Science Museum, Ueno-Park, Tokyo Japan

Editor Seiichiro Kiyota
e-mail: skiyotax@gmail.com